

# **Electronic Supplementary Information to**

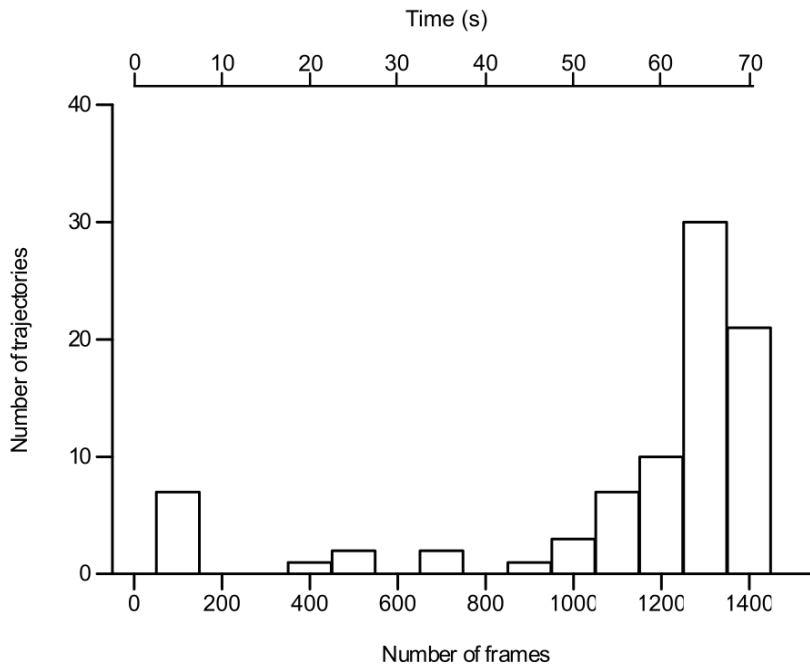
## **Extending the analogy between intracellular motion in mammalian cells and glassy dynamics**

Beatrice Corci,<sup>a,b</sup> Oscar Hooiveld,<sup>a</sup> Amalia M. Dolga<sup>a</sup> and Christoffer Åberg<sup>\*a</sup>

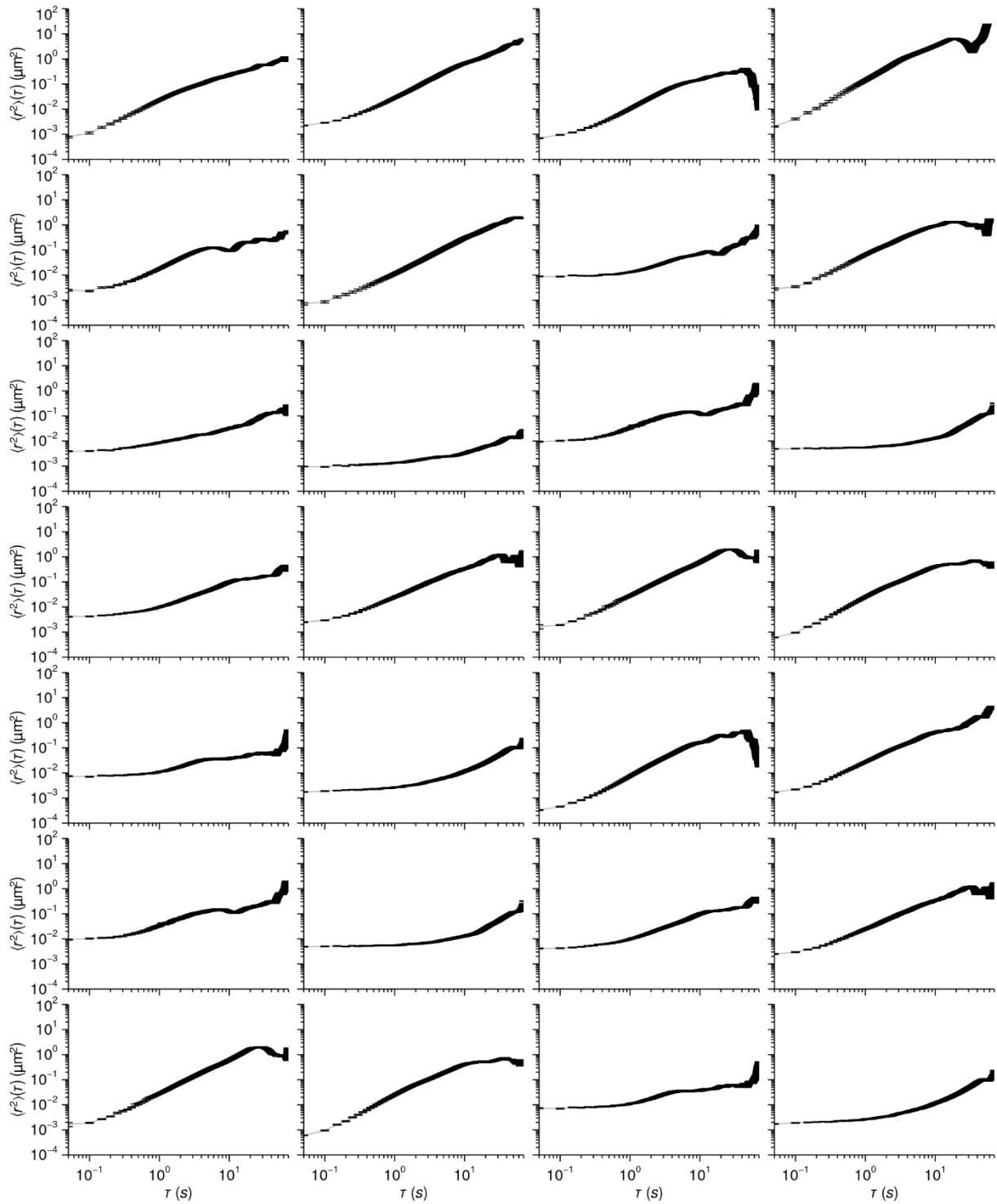
<sup>a</sup> Groningen Research Institute of Pharmacy, University of Groningen, A. Deusinglaan 1, 9713 AV Groningen, The Netherlands.

<sup>b</sup> Zernike Institute for Advanced Materials, University of Groningen, Nijenborgh 4, 9747 AG Groningen, The Netherlands.

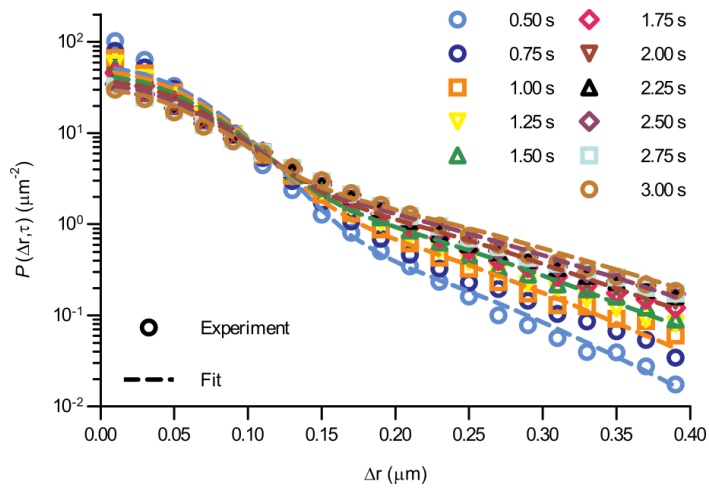
\* E-mail: christoffer.aberg@rug.nl



**Supplementary Figure S1: Trajectory length distribution for the mitochondria followed in HEK 293 cells.** Not all of the single mitochondria could be followed throughout all the frames (1400 frames every 50 ms for a total duration of 70 s) due to the presence of a dense mitochondrial network obscuring single mitochondria or the mitochondrion of interest moving to a different focal plane. The results here show the distribution of trajectory lengths both in number of frames (lower x axis) and in seconds (upper x axis). Total number of trajectories is 84 from 55 cells.

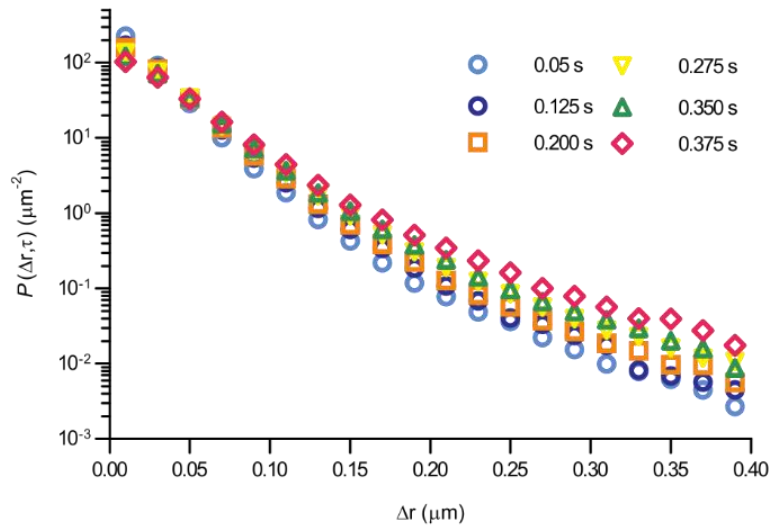


**Supplementary Figure S2: Time-averaged square displacement of example mitochondria in HEK 293 cells.** 28 trajectories were chosen at random from the set (84 trajectories from 55 cells) summarised in Supplementary Figure S1. Error bars indicate standard error of the mean.

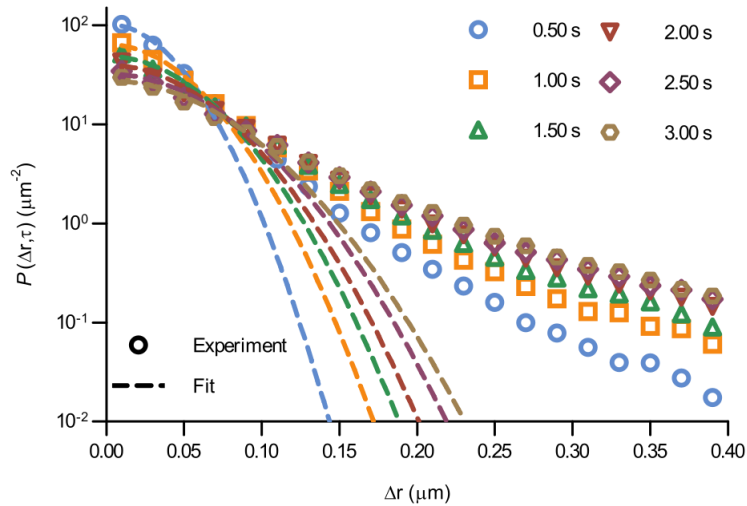


**Supplementary Figure S3: Displacement distribution of mitochondria in HEK 293 cells.**

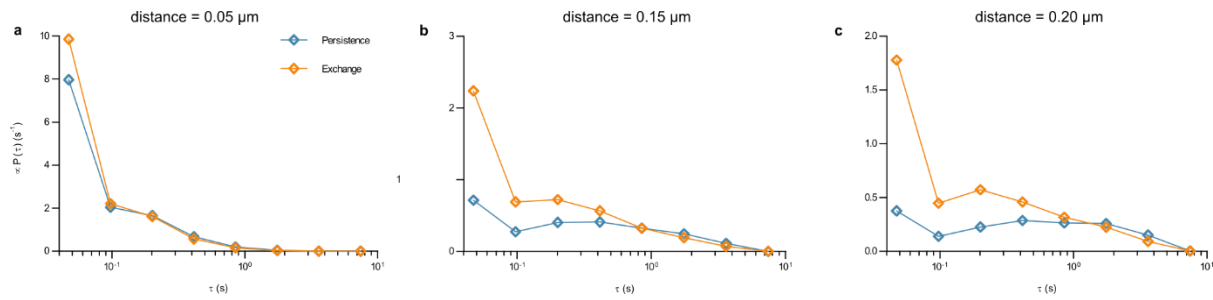
Same data as in Figure 3 of the main text, but showing more time points. (Data points) Displacement distribution of mitochondria observed experimentally for different lag times (84 trajectories from 55 cells). (Dotted lines) Fits of a model describing glassy motion<sup>1,2</sup> to the experimental data. The four fitting parameters ( $\tau_1$ ,  $\tau_2$ ,  $l$ ,  $d$ ) were ensured to be the same for all lag times.



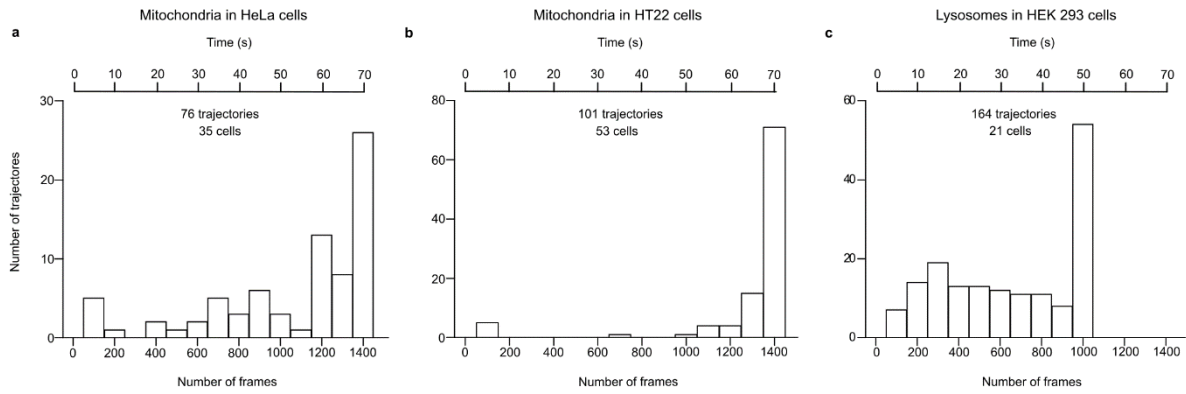
**Supplementary Figure S4: Displacement distribution of mitochondria in HEK 293 cells at shorter (0.05 to 0.5 s) timescale.** Similar data as in Figure 3 of the main text, but showing shorter timescales. (Data points) Displacement distribution of mitochondria observed experimentally for different lag times (84 trajectories from 55 cells). Note that the extent of the y axis is substantially enlarged compared to Figure 3.



**Supplementary Figure S5: The displacement distribution of mitochondria in HEK 293 cells does not follow a Gaussian displacement distribution.** (Data points) Experimental displacement distributions for a few selected times (same data as shown in Figure 3; 84 trajectories from 55 cells). (Dashed lines) Fit of a Gaussian distribution to the data. More specifically, we fitted a function of the form  $C\exp(-\Delta r^2/A)$  to the data (note that in evaluating the experimental distributions, we have excluded a factor  $2\pi\Delta r$  stemming from the two-dimensional geometry, so naturally we excluded that from the Gaussian fit as well) for  $\Delta r < 0.25 \mu\text{m}$ . For a diffusive process, the parameter  $A$  would be proportional to lag time,  $\tau$ , but we imposed no such requirement here, rather fitting each curve separately, to give the best opportunity for good fits. However, while the short length scale behaviour ( $\lesssim 0.10 \mu\text{m}$ ) is well-described by Gaussians, the tails of the distributions are clearly not. Overall, it is evident that the motion is not diffusive.

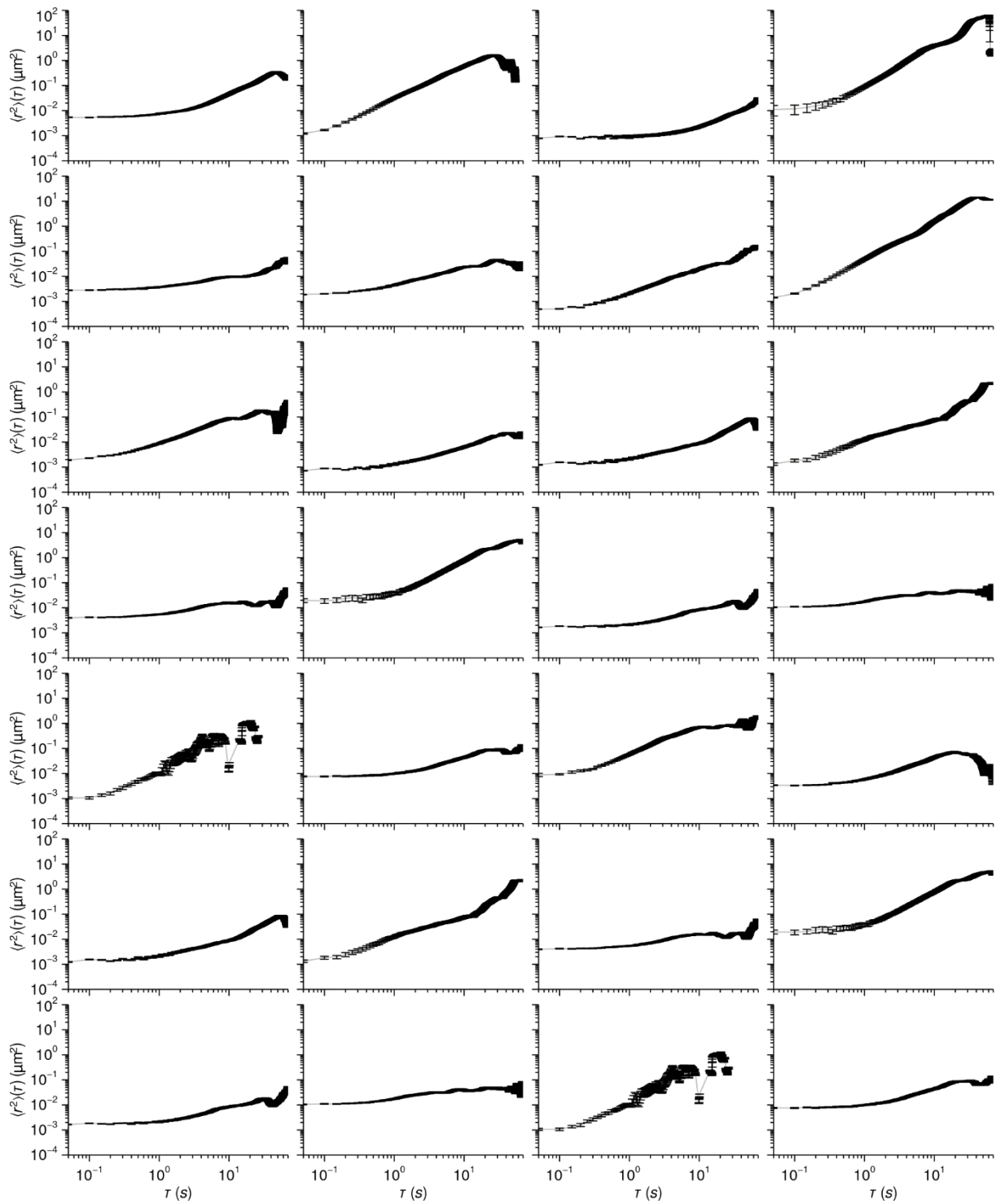


**Supplementary Figure S6: The waiting time before jumping the first time is different from the waiting time before jumping again for mitochondria in HEK 293 cells.** How long it took a mitochondrion to move a certain distance for the first time, and the time it took to move the same distance a second time having already done so once, was evaluated from the experimental data as described in Methods (84 trajectories from 55 cells). To test whether the conclusion that these two times are different was independent of the choice of jump length, we performed the calculation for the lengths 0.05, 0.10, 0.15, and 0.20  $\mu m$ . The choice of 0.10  $\mu m$  is reported in Figure 4, while the other lengths are reported here. Overall, the results show that the waiting time before jumping the first time is different from the waiting time before jumping again, regardless of the definition of what constitutes a “jump”.

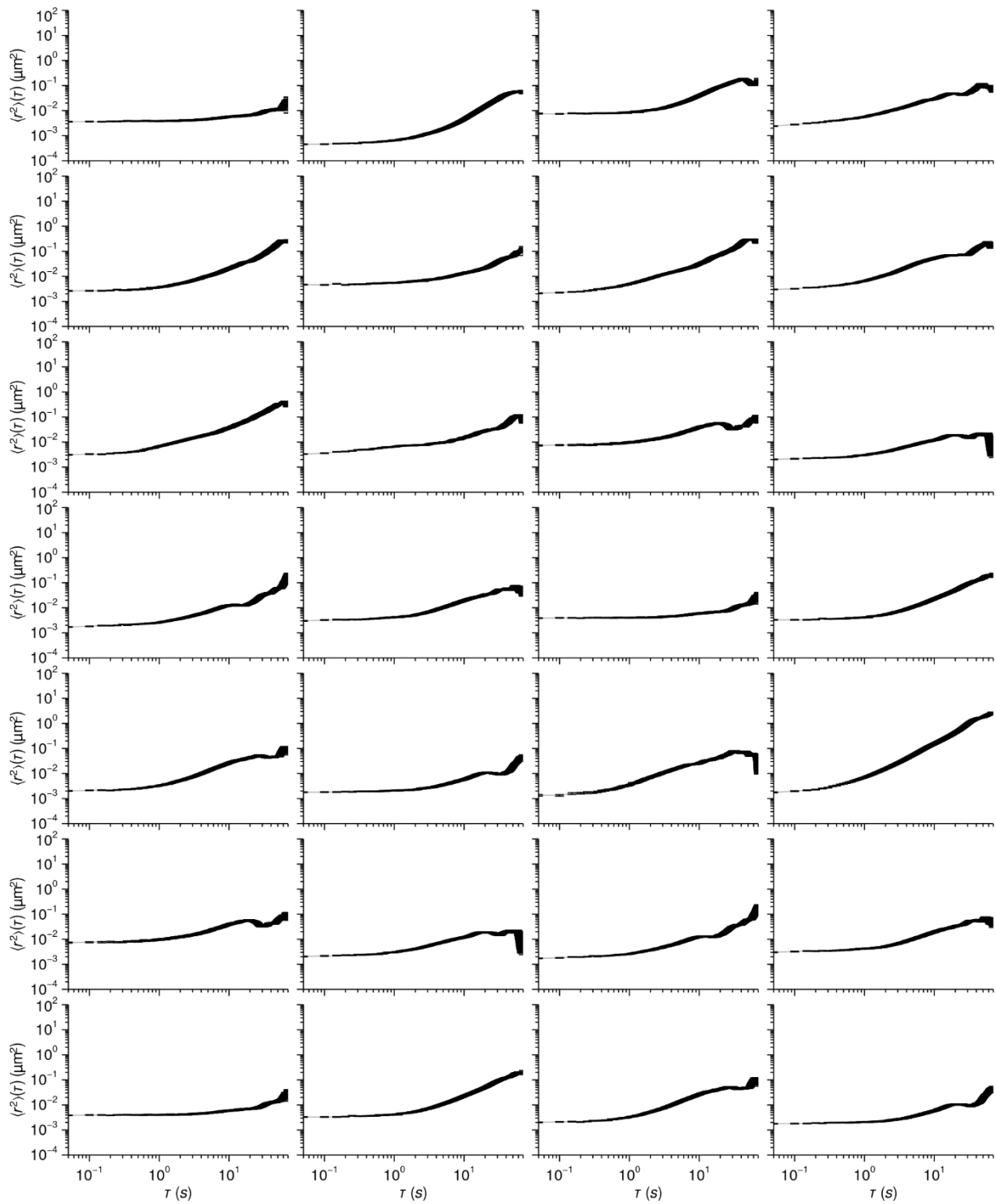


**Supplementary Figure S7: Trajectory length distribution for the organelles followed in different cell types.** Not all of the organelles could be followed throughout all the frames (1400 frames every 50 ms for a total duration of 70 s) due to the other organelles obscuring the organelle or the organelle of interest moving to a different focal plane. In the case of the lysosomes, some organelles were also lost due to photobleaching and, indeed, no lysosome was followed throughout all the frames. The results here show the distribution of trajectory lengths both in number of frames (lower x axis) and in seconds (upper x axis). Total number of trajectories and number of cells are as reported in the relevant panel.

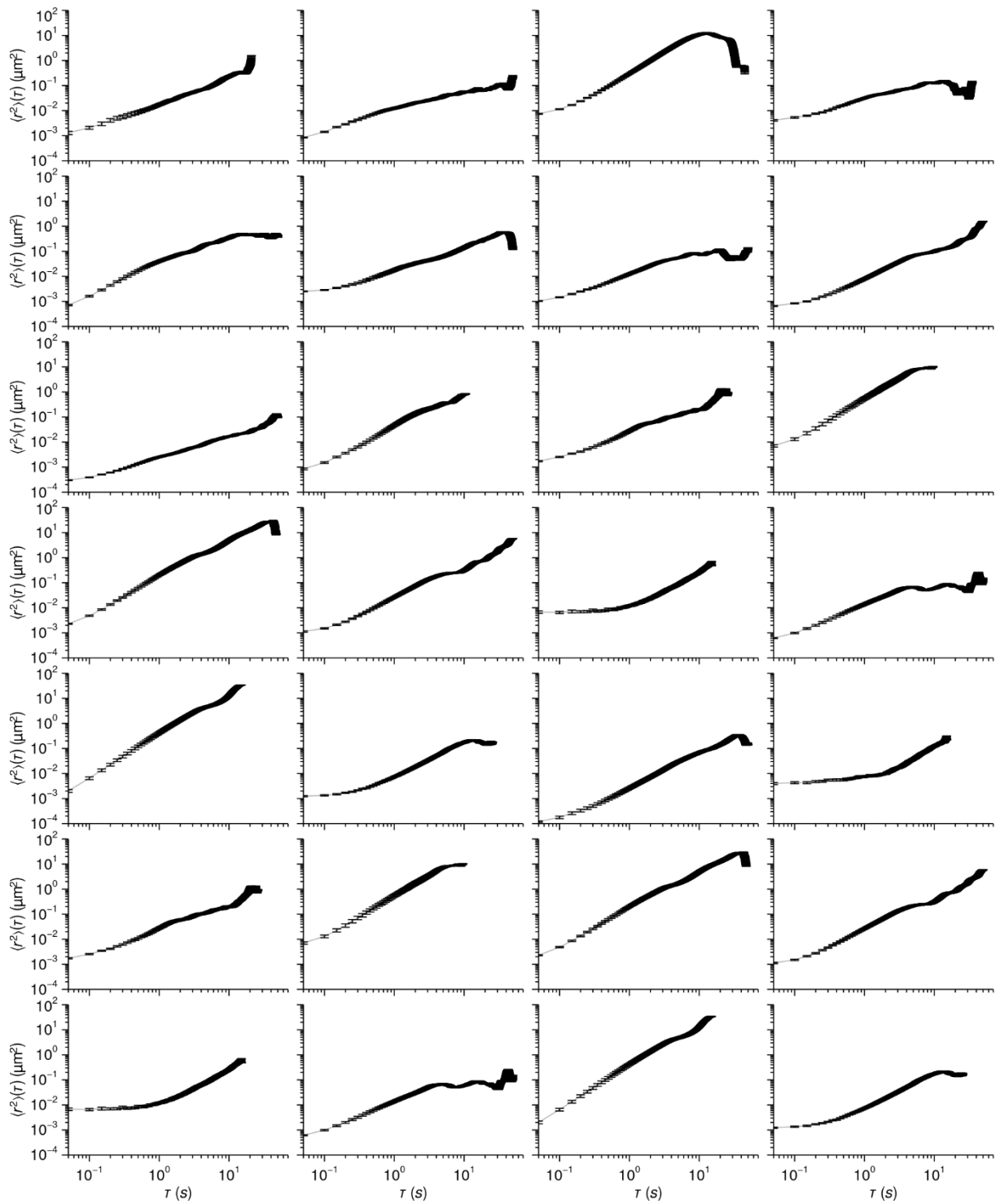




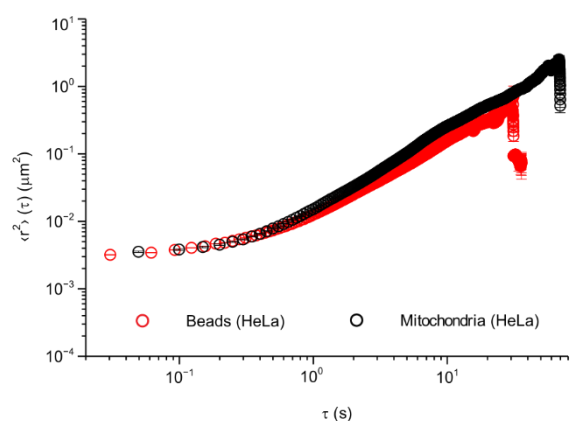
**Supplementary Figure S8: Time-averaged square displacement of example mitochondria in HeLa cells.** 28 trajectories were chosen at random from the set (76 trajectories from 35 cells) summarised in Supplementary Figure S7a. Error bars indicate standard error of the mean.



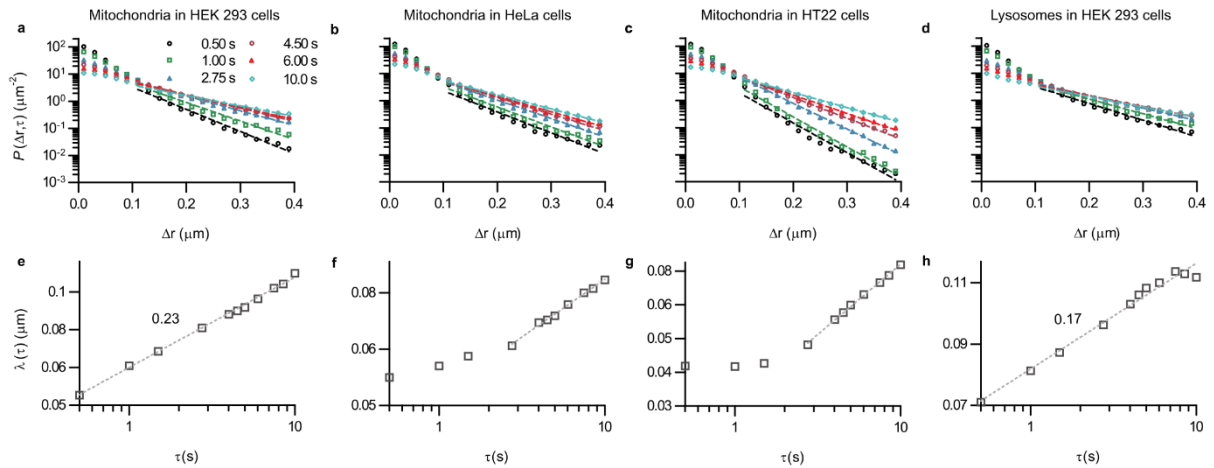
**Supplementary Figure S9: Time-averaged square displacement of example mitochondria in HT22 cells.** 28 trajectories were chosen at random from the set (101 trajectories from 53 cells) summarised in Supplementary Figure S7b. Error bars indicate standard error of the mean.



**Supplementary Figure S10: Time-averaged square displacement of example lysosomes in HEK 293 cells.** 28 trajectories were chosen at random from the set (164 trajectories from 21 cells) summarised in Supplementary Figure S7c. Error bars indicate standard error of the mean.

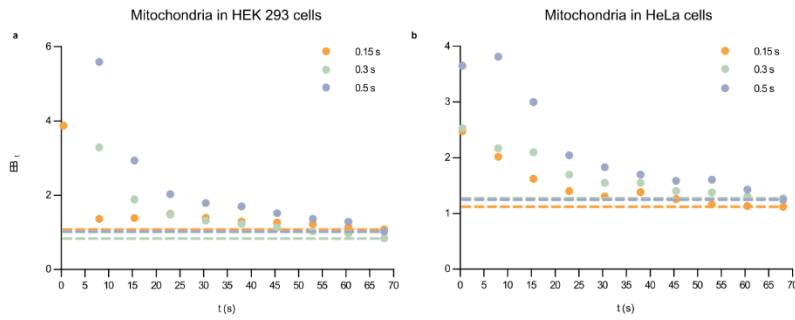


**Supplementary Figure S11: Comparison of the mean square displacement of beads within vesicles and mitochondria in the same cell type (HeLa cells).** The mean square displacement was calculated from the trajectories, averaging both over time and trajectories (ensemble). Error bars represent standard error of the mean, but most are within the symbol. (Black) Beads within vesicles, reproduced from previous literature (157 trajectories from 17 cells).<sup>3</sup> (Red) Mitochondria, from this work. Same data as presented in Figure 5a (76 trajectories from 35 cells). *N. B.* the log-log scale.

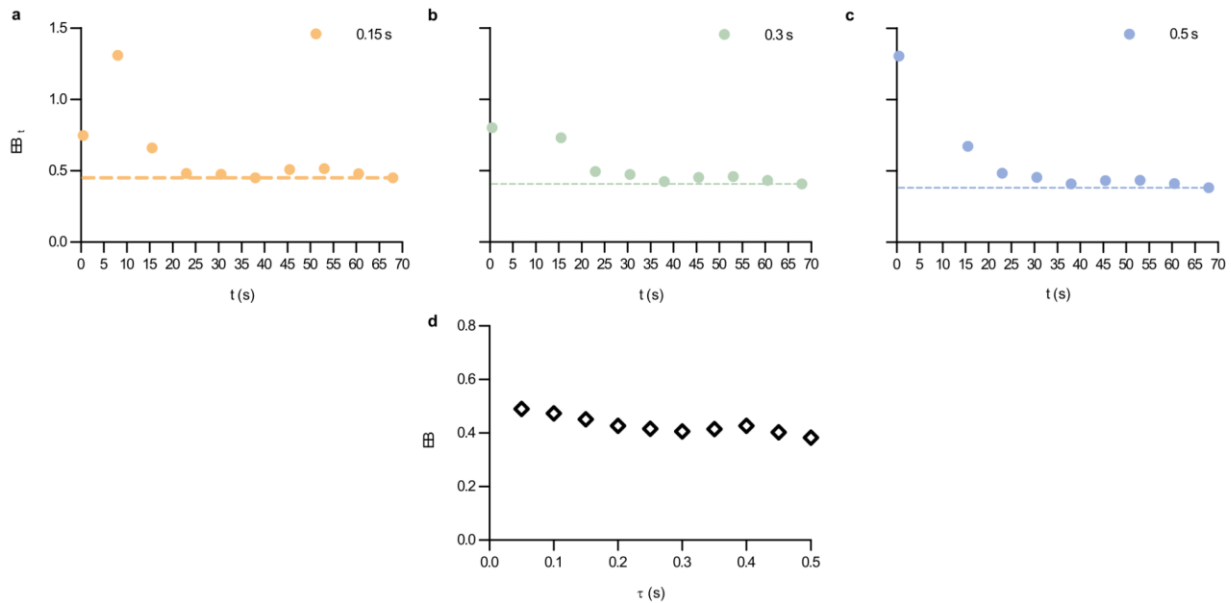


**Supplementary Figure S12: Exponential decay fitted to the displacement distributions.**

(a–d) (Datapoints) Displacement distributions with (dashed lines) fits of an exponential decay to the data for distances longer than  $0.1 \mu\text{m}$ . (e–h) The decay length extracted from the fits as a function of lag time,  $\tau$ . *N. B.* the log-log scale. (a,e) Mitochondria in HEK 293 cells (84 trajectories from 55 cells); (b,f) Mitochondria in HeLa cells (76 trajectories from 35 cells); (c,g) Mitochondria in HT22 cells (101 trajectories from 53 cells); (d,h) Lysosomes in HEK 293 cells (164 trajectories from 21 cells). For the mitochondria and lysosomes in HEK 293 cells, the decay length roughly follows a power law with an exponent of 0.23 and 0.17, respectively. However, the other two systems do not show a power law behaviour, at least for the full time interval. Additionally, the power law exponent varies between the systems studied here, and is also different from the exponent of 0.27 found for beads in HeLa cells in our previous work.<sup>3</sup>

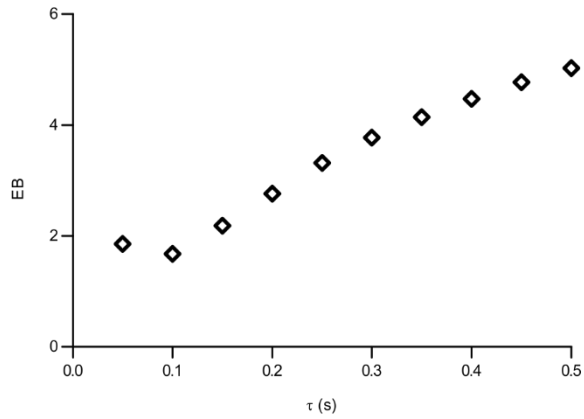


**Supplementary Figure S13: Attempt at characterising ergodicity breaking of mitochondria in HEK 293 and HeLa cells.** We characterised whether their motion was ergodic or not using the ergodicity breaking parameter, EB, introduced in previous literature.<sup>4-6</sup> This parameter in general depends on lag time,  $\tau$ , and is defined as an infinite time limit. We started by evaluating a time-dependent version of the parameter,  $EB_t$ , that is, we quantified the parameter which in the infinite time limit becomes the ergodicity breaking parameter, EB. (Datapoints) Parameter,  $EB_t$ , that tends to the ergodicity breaking parameter in the infinite time limit for three exemplar lag times,  $\tau = 0.15, 0.30$  and  $0.50$  s. (Dashed lines) Value after 70 s to visualise the convergence of  $EB_t$ . (a) Mitochondria in HEK 293 cells (84 trajectories from 55 cells); (b) Mitochondria in HeLa cells (76 trajectories from 35 cells). In both cases, we do not see a clear convergence, implying that we are not able to define the ergodicity breaking parameter.



**Supplementary Figure S14: The motion of mitochondria in HT22 cells is non-ergodic.**

We characterised whether their motion was ergodic or not using the ergodicity breaking parameter,  $EB$ , introduced in previous literature.<sup>4–6</sup> This parameter in general depends on lag time,  $\tau$ , but for ergodic motion it is independent of lag time and equal to 0. Furthermore, this parameter is defined as an infinite time limit, so we started by evaluating a time-dependent version of the parameter,  $EB_t$ , that is, we quantified the parameter which in the infinite time limit becomes the ergodicity breaking parameter,  $EB$ . The results are based on 101 trajectories from 53 cells. (a–c) (Datapoints) Parameter,  $EB_t$ , that tends to the ergodicity breaking parameter in the infinite time limit for three exemplar lag times,  $\tau = 0.15, 0.30$  and  $0.50$  s. (Dashed lines) Value after 70 s to visualise the convergence of  $EB_t$ . The fact that the values remain roughly the same after 20–30 s suggests that using  $EB_t$  for  $t = 70$  s is a reasonable approximation of the ergodicity breaking parameter  $EB$ , which, in principle, is only defined as the infinite time limit. (d) Ergodicity breaking parameter as function of the lag time,  $\tau$ . Only lag times where we observed a convergence (as in panels a–c) where included. For all lag times, we observe an ergodicity breaking parameter close to 0.4. This is clearly distinct from 0, showing that the motion is non-ergodic.



**Supplementary Fig. S15: The motion of lysosomes in HEK 293 cells is non-ergodic.** We characterised whether their motion was ergodic or not in the same way as described in Supplementary Figure S14, including only lag times where we observed a convergence. The results are presented in terms of the ergodicity breaking parameter as function of the lag time,  $\tau$ . We observe an ergodicity breaking parameter that is different from 0 for all lag times, showing that the motion is non-ergodic.



## References

- 1 P. Chaudhuri, L. Berthier and W. Kob, *Phys Rev Lett*, 2007, **99**, 060604.
- 2 P. Chaudhuri, Y. Gao, L. Berthier, M. Kilfoil and W. Kob, *J Phys: Condens Matter*, 2008, **20**, 244126.
- 3 C. Åberg and B. Poolman, *Biophys J*, 2021, **120**, 2355–2366.
- 4 Y. He, S. Burov, R. Metzler and E. Barkai, *Phys Rev Lett*, 2008, **101**, 058101.
- 5 S. Burov, J. H. Jeon, R. Metzler and E. Barkai, *Phys Chem Chem Phys*, 2011, **13**, 1800–1812.
- 6 R. Metzler, J.-H. Jeon, A. G. Cherstvy and E. Barkai, *Phys Chem Chem Phys*, 2014, **16**, 24128–24164.